ON THE ANALYSIS OF COMPUTER VISION AND ULTRASOUND BASED TECHNIQUES FOR THE IN-SERVICE INSPECTION OF AERONAUTICS PARTS PRODUCED BY ADDITIVE LAYER MANUFACTURING (ALM)

Nekane Galarza, Benjamín Rubio, Arantza Bereciartua[1], Iván Lozano, Jaime Gascón, Garbiñe Atxaga, Jose Pérez

Fundación Tecnalia Research & Innovation. C/ Geldo, 700, 48160 Derio (Bizkaia) Spain. [1]aranzazu.bereciartua@tecnalia.com, tfno. 664107703

Received: 23/Dec/2019 – Reviewing: 02/Jan/2020 -- Accepted: 10/Mar/AA - DOI: http://dx.doi.org/10.6036/9622

1.- INTRODUCTION

This paper describes the work accomplished under the Bionic Aircraft project founded under H2020 framework. It aims at reducing emissions in the aviation industry [1].

ALM can produce more cost-effective and lighter parts. Mainly, to manufacture metallic parts, Laser Beam Melting (LBM) is used. Melting metal powders layer by layer offers geometrical freedom that cannot be achieved otherwise. Moreover, parts produced by ALM fulfil different product requirements within a single building process, saving process steps and enabling lower costs compared to the conventional production [2]. Nowadays, the interest in ALM is increasing [3-5]

Several materials can be used in ALM. The use of Ti alloys, for example, implies a weight reduction of 40% (compared with one Al aircraft part manufactured by conventional milling) and the wasted product is less than 10%. In case of Al-Li based alloys, the weight reduction is even higher (50%) [1]. Steels, Ni- and Co-based superalloys and Al alloys are also used.

One of the pending actions is the development of new in-service NDT strategies of parts produced by ALM. In-service inspection involves challenges like the uncertainty of the inner inspection of a layered material and the surface quality, the lack of accessibility, and the expected defects produced by in-service conditions.[6]

Typical defects (such as pores or cracks) produced with ALM are listed in some research articles [6, 7] but they are assumed to be detected in-process or in-line. So that, only defects that appear or grow during in-service life of the part will be searched in the scope of this work, which are different from the defects detected in previous stages. The defects will be: surface damages, fatigue cracks that appear on the surface and grow inward, and internal cracks, which could grow due to fatigue, from a “seed” like small hot-cracks [8], undetected during in-process or in-line because its size was acceptable.

This work is focused on assessing the inspection feasibility of bionic parts made of AlSiSc, selecting the most suitable NDT methods, according to the damage information obtained by a fatigue life prediction study.

2.- MATERIALS AND METHODS

In this section, different steps are described to carry out a screening of potential applicable technologies.

2.1. 1ST SCREENING: BIBLIOGRAPHIC ANALYSIS.

Large number of references were found in the bibliography, being X-ray based techniques and ultrasound (US) the most cited to detect inner defects. For sub-superficial defects detection, Thermography and Eddy Current were the most referenced. 3D sensors are also used for quality control in manufacturing [9]. Similar parts are inspected by using both X-ray Computed Tomography (CT) (internal defects) and Dye Penetrants (surface defects).
The most relevant physical properties of ALM materials provide a clue to select technologies to inspect inner defects. A grain size of ~50µm [10] is obtained with cellular or columnar grains, depending on the built direction. Considering, in terms of ultrasonic

inspection, that the grain noise is a problem when the grain size of the material is larger than $\lambda/10$, the relation $\lambda=c/f$ with c=6250m/s (longitudinal velocity of Al), determines that the upper limit for the frequency is 12,5-15MHz. In terms of macrostructure, grain size of ~200µm [10] is obtained.

Although CT seems to be the most suitable NDT method, a priori, it cannot be applied for in-service inspection, because access to both sides of the sample is required. Likewise, any method involving oversized or heavy equipment are not viable due to accessibility limitations. US seems to be suitable to detect inner defects, since small equipment and one inspection access are required. In terms of surface/sub-surface defects, Thermography and Computer Vision (CV) will be also considered.

2.2. 2ND SCREENING: LAB-SCALE TESTING ON SIMPLE REFERENCE SPECIMENS.

The selected technologies were tested at lab-scale on simple specimens, made of $AlSi_{10}Mg$ (similar to AlSiSc). Some defects were induced.

2.2.1. Computer Vision (CV)

Different CV-based solutions were tested. **Laser Triangulation** was performed with commercial 3D sensor Gocator 2370 (Resolution: 0,275mm (XY); 0,055mm (Z)). This resolution was not enough to obtain great contrast to detect notches. Although there are systems with higher resolution, time to inspect the same area could take much longer, mainly in case of complex part inspection.

Structured Light 3D Scanner was performed with Gocator 3110 (Resolution: 0,100mm (XY); 0,035mm (Z)), but the resolution was not high enough to detect any defect.

Diffused Dome Light (Domo) diffuses light at all angles. This is the reason why a target with a complex shape can be uniformly lit, eliminating hotspots. Results obtained showed great contrast to detect notches (*Halcon* vision library was used), though areas with spurious artefacts/false positives appear.

2D Darkfield was tested by using white and red lights. Better results were obtained with white light illumination, but both techniques showed good results. Irrelevant artefacts on the surface were detected, so posterior image processing algorithm is required.

<table>
<tr><th colspan="2">Specimen</th><th colspan="2">Artificial defects</th></tr>
<tr><th>Nº</th><th>Dimension [mm]</th><th>Lay-out (defects induced by EDM)</th><th>Sizes [mm]</th></tr>
<tr><td>1</td><td>100x100x18,3*</td><td rowspan="3"> 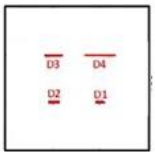

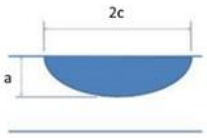
</td><td rowspan="3"><table>
<tr><td>D1</td><td>a=0,5</td><td>2c=1,5</td></tr>
<tr><td>D2</td><td>a=1,0</td><td>2c=3,0</td></tr>
<tr><td>D3</td><td>a=2,0</td><td>2c=6,0</td></tr>
<tr><td>D4 (Nº1,2)</td><td>a=5,0</td><td>2c=15,0</td></tr>
<tr><td>D4 (Nº3)</td><td>a=3,0</td><td>2c=9,0</td></tr>
</table></td></tr>
<tr><td>2</td><td>100x100x16*</td></tr>
<tr><td>3</td><td>100x100x4*
* initially defined thicknesses: 19 and 5mm. Due to ALM, approximate dimensions have been obtained.</td></tr>
</table>

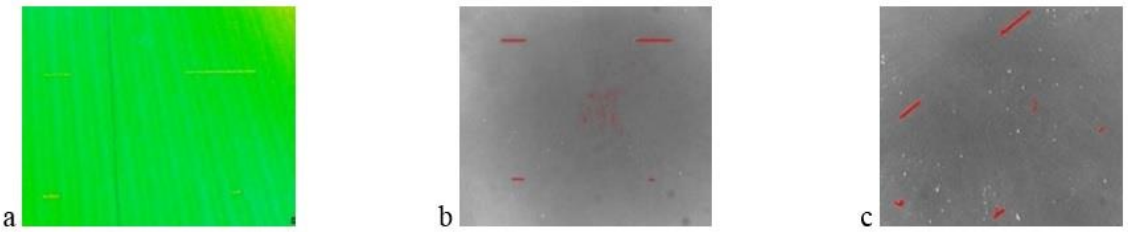

Figure 1. Manufactured specimens; and the results obtained with a) Structured Light, b) Domo, c) Darkfield.

2.2.2. Thermography (T)

Internal defects were induced in testing specimens, ones simulated by both Flat Bottom Holes (FBH) and others inducing them during the manufacturing process.
The samples were inspected by active Infrared Thermography (IRT) (FLIR SC5000). Three different stimulation approaches were used: continuous optical, pulsed optical and inductive, using a halogen lamp (1KW), a flash lamp (6KJ) and induction coils (15A-10KW), respectively.
Thermography showed no good response to detect internal cracks. Many indications were detected over the entire surface of the specimens that did not correspond to real defects. This could have been due to the specific internal structure of the material, with high levels of porosity and thermal diffusivity. High diffusivity and porosity distribute the heat rapidly over the material, spreading the heat originated in the defects so quickly that it is not possible to detect any defect before dissipating all the heat even with a high-speed camera.

2.2.3. Ultrasound (US)

US was tested over the previous specimens and others. Some of them were used to measure acoustic properties (attenuation, sound velocity and signal-to-noise ratio) and to study the effect of the surface quality; and the rest, to verify the capability to detect internal defects.

Single element pulse-eco testing was performed at this stage by using contact transducers. Straight angle transducers in the range of 2,25–20MHz were used and wedges of 45º. Delay lines were also employed. A wide range of frequencies was tested considering the common frequencies used in the bibliography, the grain size and the shape and location of defects.

Regarding sound velocity, higher values than steel or Al were obtained (C_L=6581m/s, C_S=3271m/s). Acoustic attenuation tests showed low values for all frequencies, obtaining higher values as frequency increased. Attenuation derived from the surface quality showed huge reduction of echo amplitudes, which was higher as frequency increased (6 to 60 times smaller). Despite the grain size and layered structure, good signal-to-noise ratio values were obtained (23-49dB) by optimizing the transmission and receiving (filtering) parameters.

In terms of defect detection, best frequencies were between 10-20MHz. All notches and all FBH ≥ ∅0,5mm were clearly detected (more hardly those FHB closer to the surface; 2-3mm). In Figure 2, it can be seen that echoes coming from smaller defects and defects near surface are less clear.

Specimen		Artifictial defects		
Nº	Dimensions [mm]	*X-Y* Layout	Shape in other planes or detail	Sizes
N	100x100x3	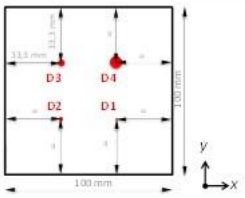	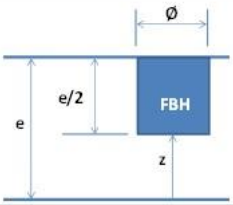	Ø (mm): D1 0,2; D2 0,5; D3 1,0; D4 2,0
N+1	100x100x18,2			
N+2	100x100x3	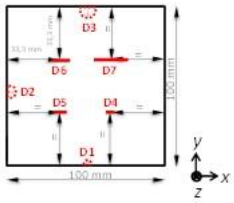	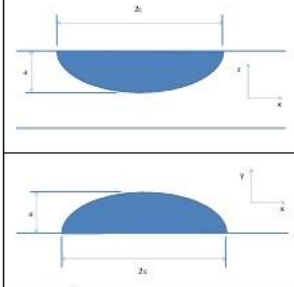	a(mm) / 2c(mm) / SURFACE: D1 0,5 / 1,5 / Side; D2 1,0 / 3,0 / Side; D3 2,0 / 6,0 / Side; D4 0,5 / 1,5 / Wide (one); D5 1,0 / 3,0 / Wide (one); D6 2,0 / 6,0 / Wide (one); D6 3,0 / 9,0 / Wide (one)

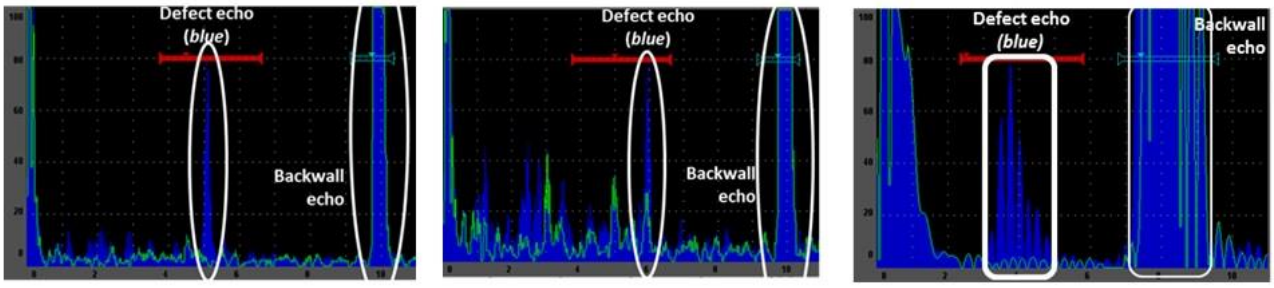

Figure 2. Some specimens manufactured for US and the signals obtained: (Left) Nº N, D2. (Centre) Nº N+1, D1. (Right) Nº N+2, D2.

The technologies were evaluated in 3 aspects: the influence of the internal structure of the material; the influence of the surface quality; and the detectability of certain expected type and size of defects. Additionally, accessibility and the maturity level were also considered. Technologies, like Terahertz and Deflectometry were discarded because of its expensiveness and the huge size of the transducers, respectively. Regarding US, Electro Magnetic Acoustic Transducer (EMAT) was discarded due to large size of transducers. Laser US was also discarded because its limitations on penetration capacity, large size of the equipment and expensiveness. A customized Small Footprint Phased Array Transducer (SFPAT) (10MHz/20elements/pitch 0,31mm) along with two 0° (0,5mm and 12mm thick) wedges and one of 45° were manufactured based on the obtained results with mono element transducers. It was used in the experiments involved in 3rd and 4th screenings.

2.3. 3RD SCREENING: LAB-SCALE TESTING ON COMPLEX REFERENCE SPECIMENS.

The selected technologies were tested in complex shaped specimens, in which some of them, artificial defects were induced. The type and shape of the specimens were selected according to the results of the fatigue life prediction study.

This analysis, whose main objective is to establish the expected fatigue life, is based on identifying points where the probability of developing fatigue failures is maximum (critical zones). The categorization of the different zones is carried out based on the stress ranges derived from the external efforts and the NDT crack size threshold. Considering that fatigue cracks propagate according to an exponential law, it is crucial to develop an NDT system with a low damage size threshold to assure a long fatigue life. As a result, critical zones were identified, and four different crack types were considered: surface, corner, through and embedded. According to these data, complex shaped specimens were defined, and defects were artificially induced. Depending on the defect type and its location, one of two technologies (CV or US) was assigned to inspect each defect.

2.3.1. Computer Vision (CV)

Laser Triangulation based 3D Scanner, Domo and Darkfield were tested. As a result, Domo and Darkfield were the most suitable technologies. Laser Triangulation based 3D Scanner was not able to inspect cracks (Figure 3).

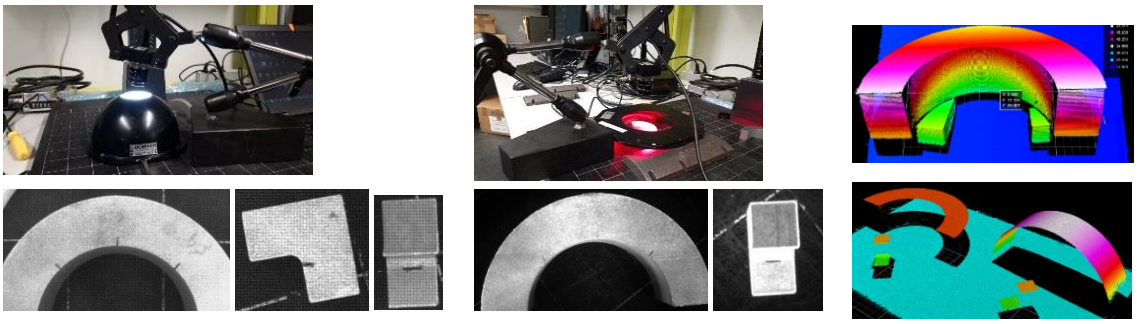

Figure 3. Images obtained with: Domo (Left); Darkfield (center); Laser Triangulation-based 3D system (right)

2.3.2. Ultrasound (US)

The inspection with US was not performed in these specimens, because they were not representative due to the complexity of the final demonstrator, where the Inspection Areas (IA) regarding critical zones are highlighted. Simulations of the ultrasonic beam propagation with Beamtool 9© were done to identify non-inspectable zones for each transducer. In conclusion, angular single element transducer and specially the SFPAT seem to offer the best ultrasonic coverage in all zones.

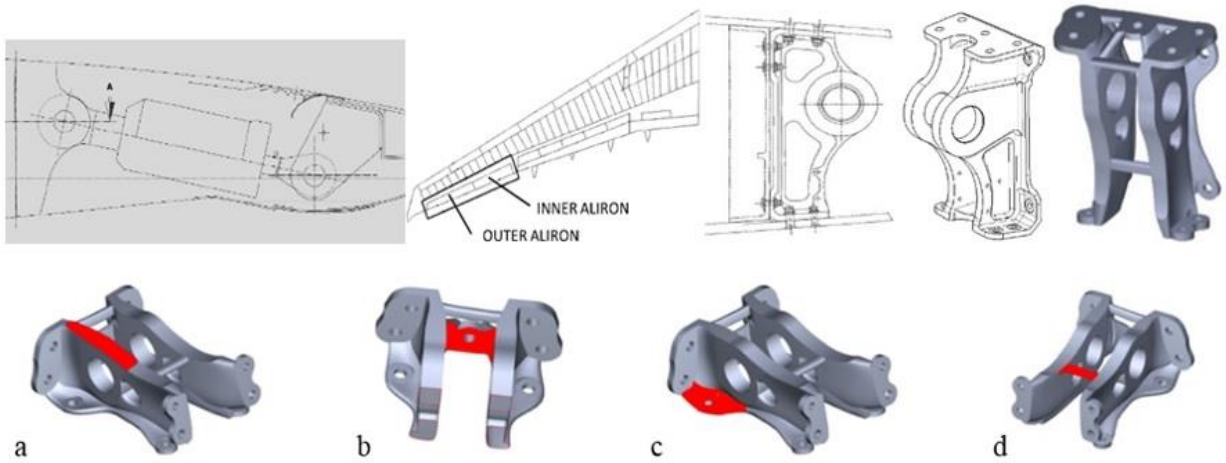

Transducers	Critical zones					
	Z1	Z2	Z3	Z4	Z5	Z6
Straight angle-single element	R	R	R	NO*	NO	NO
Angular single element	OK	OK	OK	OK	NO	OK
PA – 0º / Wedge	R/OK	R/OK	R/OK	NO/OK	NO/OK	NO/OK

**Except one, which works properly; R: Regular (some non-inspected areas)*

Figure 4. Design and position in the wing and assembly of the new bionic part, together with inspection Areas: a) Z1, Z2, Z3; b) Z4; c) Z6; d) Z5. Usability of each transducer

The objectives of these tests were: 1) to evaluate the coverage zone of the selected technologies in the areas with most complex geometry and the accessibility, and 2) to evaluate the feasibility of detecting the critical defects.

In addition, as soon as the final material (AlSiSc) was available, simple shaped specimens were manufactured and acoustic properties of these specimens were measured to check if the change of the material required significant changes in inspection strategies. In terms of sound velocity, the obtained results were similar to $AlSi_{10}Mg$ (C_L=6448m/s-C_S=3420m/s). Acoustic attenuation, however, seemed to be lower, specially at high frequencies. Good (similar) signal-to-noise ratio values we also obtained. In summary, two materials showed similar acoustic behaviour, that indicates that the results obtained with $AlSi_{10}Mg$ can be extrapolated to AlSiSc.

2.4. 4TH SCREENING: LAB-SCALE TESTING ON COMPLEX DEMONSTRATOR.

A study of the potential methods in the most critical areas of the final demonstrator was started. By means of a 3D printer the other elements surrounding the bracket have been simulated. At this point it is not enough with the feasibility of the solution for cracks detection, but also accessibility issues are key questions. Some cracks were inferred in the available bracket for testing purposes. Results are described in next section.

3.- RESULTS

3.1. COMPUTER VISION

The darkfield lighting strategy has been skyped due to the geometry of the bracket and the need of placing the light with a specific low angle pose. So, **3D structured light** and **2D diffuse light** strategies have been evaluated.

For the **3D structured light-based inspection**, the commercial device used for these tests has been the Gocator ™3110. Its accuracy on the XY plane is 100 microns and on the Z plane 6 Microns.

On each zone, several captures have been done considering different incidence angles, trying to find the best configuration. Next, MvTec Halcon ™ commercial processing library has been used to process the images. By the modification of the incidence angle, the defects on the central side of the surface has been clearly identified. It must be remarked that this strategy does not avoid some false defects identification, due to the roughness of the surface. This trouble is reduced in the areas where the roughness of the surface is smoother. The results are not satisfactory enough.

For the analysis of **diffuse illumination**, the chosen commercial device is the model UI-3080CP ™ of IDS manufacturer. Its IMX250 sensor has a resolution of 2456 x 2054 pixels. Following the same process than with the 3D systems, the task has been split up, working on the different zones so to look for the best configuration for each one. The lighting system has been a Dome, which illuminates objects from camera axis to all directions, providing great amount of uniform light that eliminates brightness and shadows. At the same time, the exposition time, the distance to the sample and the image contrast are different parameters which must be tuned together to obtain a suitable performance.

The first objective was to check if the system can distinguish the cracks in the outer corners of the lug. As it has been stated, different acquisitions are made of the zone with different angles of attack. Besides, every acquisition and angle of attack requires different exposure times, ranging from 100 to 300 ms. The reason is that the different angles may cause occlusion zones or create shadows. For every angle the more optimum exposure time has been selected. This exposure time allows to have a good quality image in terms of high contrast.

In the in-service process every position modification will have the proper parameters to be applied. There is no problem in automatizing this. Over the final AlSiSc demonstrator several cracks have been induced in the different zones. The summary of the distribution of the cracks and the sizes is gathered in the following figure:

LUG	HOLE	SURFACE	STRESS CONCENTRATOR	THIN WALL
		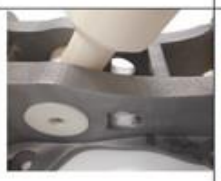		
Equidistant placement. Size: 1 x 0.2 x 1 millimetres	1 set of 3 cracks. Size (central area) 1.5 x 0.2 x 0.5 millimetres. 2 sets of 3 cracks. Size (lateral corners) 1 x 0.2 x 1 millimetres.	6 cracks. 20 to 30 millimetres distance. Central area 1.5 x 0.2 x 1 millimetres 2 sets of 6 cracks distributed as the previous ones. Size (both corners) 1 x 0.2 x 1 millimetres	1 crack. Size (central area of the corner) 3 x 0.2 x 1 millimetres 2 cracks. Size (edges of the corners) 1 x 0.2 x 1 millimetres	4 cracks. Size (centre of each join) 3 x 0.2 x 1 millimetres 4 cracks. Size (corner of each join) 1 x 0.2 x 1 millimetres

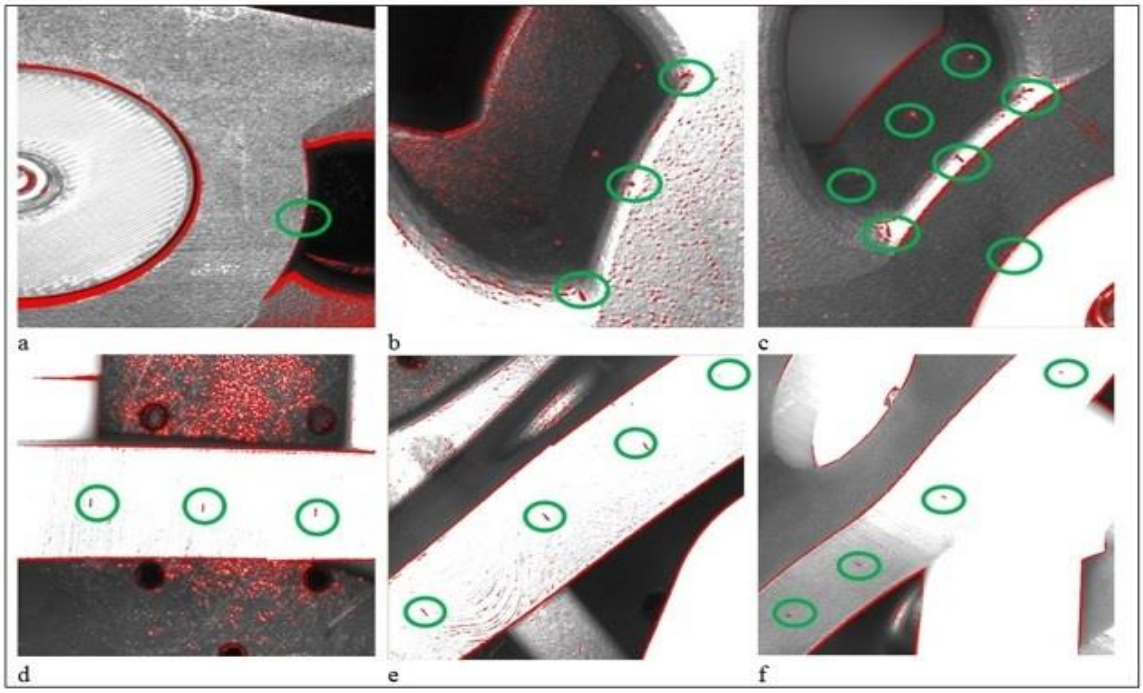

Figure 5. Cracks induced over the final demonstrator and Results for diffuse illumination layout and the inspection algorithm in the "hole" zone: a) camera at 0º; b) 15º; c) 30º; and in the "surface" zone: d) camera at 0º; e) 15º; f) 30º.

No good results were obtained for zones "lug", "stress concentrator" and "thin wall". Accessibility is a problem.

3.2. US TECHNIQUES

The final set of inspection parameters, along with four focal laws for the Small Footprint Phased Array Transducer (SFPAT) were established. The focal laws involve S-Scans, L and S waves, 16 active elements per law, steering angles from -30° to +70° (1° step) and focal distances from 5mm to ∞ depending on the specific law. Besides, the final transducer selection comprises those from 5MHz to 15MHz.

Based on the conclusions stated by the life prediction study, a set of reference defects having the maximum admissible sizes (∅1mm internal crack and 1x3mm surface cracks) were machined directly on the final demonstrators made of AlSiSc and AlSi10Mg.

Each of those defects is representative from each critical zone under the worst possible situation and inspection point of view (worst access, orientation, etc.).

All the reference defects were detected, except one located in the Z6. The steering capability and beam forming of the Phased Array technique and the small sizes of the transducers used (requiring small contact surfaces) were key to succeed in the detection in zones with difficult access and complex geometry. The only undetected defect was located on inner surface of the bolt hole because of the lack of access surface and its irregular shape. A detection summary is gathered in figure 9.

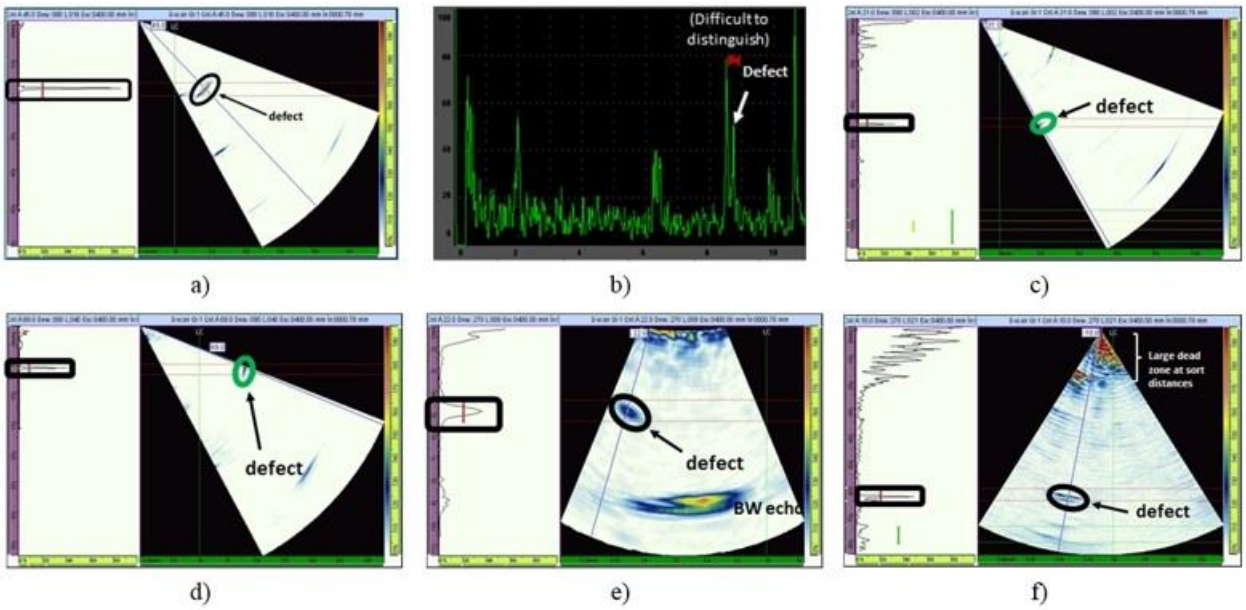

ULTRASONIC INSPECTION VIABILITY			
CRITICAL ZONE	*DEFECT*	*DETECTABILITY*	*TRANSDUCER USED*
Z1	Z1-S-1	**YES**, clearly	SFPAT-W45°
	Z1-S-2	**Very hardly**	All (T3)
	Z1-S-3	**YES**, clearly	T2, T3, T4
	Z1-E-2 /'	**YES**, but hardly	SFPAT-W45°
	Z1-E-1/'	**YES**, clearly	SFPAT-W45°
Z2	= Z1-E-1/'	**YES**, clearly	SFPAT-W45°
Z3	Z3-E-1/'	**YES**, clearly	SFPAT-W45°
Z4	Z4-E-1/'	**YES**, but hardly	SFPAT-W0°-1
Z5	Z5-E-1/'	**YES**, clearly (*)	SFPAT-W0°-2
Z6	Z1-C-1'	**YES**, clearly (**)	SFPAT-W45°
	Z1-S-1/'	**NO**	All

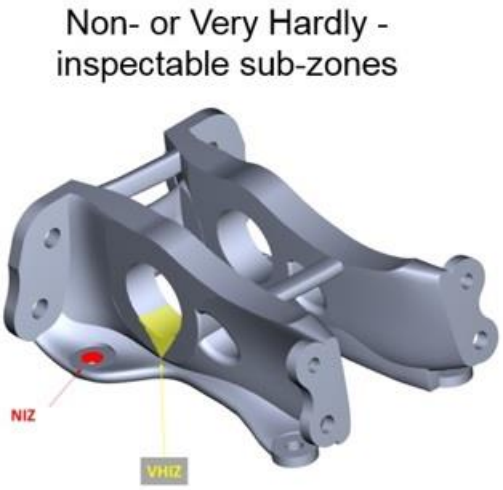

Figure 6. a) LUG: Surface crack (upper); b) LUG: Surface crack (lower); c) Between LUG and HOLE: embedded crack; d) FREE SURFACE: embedded crack; e) STRESS CONCENTRATOR: embedded crack; f) THIN WALL: embedded crack.

4.- ANALYSIS OF RESULTS AND CONCLUSIONS

As main conclusion of this work, a combination of US and CV based technologies was founded as the most suitable strategy to in-service inspection of these ALM bionic parts. Computer Vision techniques will provide information of surface cracks whereas US will allow to detect internal defects.

Regarding **Computer Vision technologies**, 3D structured light and 2D camera with diffuse illumination strategies have been evaluated. A combination of both CV technologies is suitable for the location of surface cracks over ALM parts. Due to the accessibility issue, specific angles of attack and exposure times have been defined. Later, algorithm is applied. This procedure can be automatized with a robotic arm that should carry out the inspection in the piece. The robotic arm must follow an established trajectory for the inspection of all the zones. Every time it is in position, it launches the execution of the processing algorithm to detect the cracks. This process does not require human interaction.

In terms of **US inspection**, Small Footprint PA transducers seem to be the most suitable ones (thanks to their steering and beam forming capabilities along with the small size), because of the common high complex geometry of the ALM parts. Ultrasonic technique is feasible to inspect most of the zones of the demonstrators, internal defects can be detected as well as the surface cracks on inaccessible surfaces, two small non-inspectable zones have been found in our specific demonstrator.
The future work relies on: 1) the use of flexible wedges/contact faces for SFPAT that may improve the coupling between the transducer and the part on complex shaped surfaces and therefore, the obtained signals; 2) the latest developments in downsizing the devices involved in LUS and EMAT may make viable the use of these without a coupling agent; 3) the development aimed toward the automation of the scanning paths.

REFERENCES

[1] Increasing resource efficiency of aviation through implementation of ALM technology and bionic design in all stages of an aircraft life cycle. BIONIC Aircraft Project. Recovered from: https://bionic-aircraft.eu/
[2] Laumer, T., Karg, M., & Schmidt, M. (2012). Laser beam melting of multi-material components. *Physics Procedia, 39, 518-525.*
[3] Zhang, Q., Xie, J., Gao, Z., London, T., Grif, D., Oancea, V., 2019. A metallurgical phase transformation framework applied to SLM additive manufacturing processes. Mater. Des. 166. doi: https://doi.org/10.1016/j.matdes.2019.107618
[4] Conde, F.F., Escobar, J.D., Oliveira, J.P., Jardini, A.L., Filho, W.W.B., Avila, J.A., 2019. Austenite reversion kinetics and stability during tempering of an additively manufactured maraging 300 steel. Addit. Manuf. 29, 100804. doi: https://doi.org/10.1016/j.addma.2019.100804
[5] Angel, M., Arredondo, Z., Zavala-arredondo, M., London, T., Allen, M., Maccio, T., Ward, S., Grif, D., Allison, A., Goodwin, P., Hauser, C., 2019. Use of power factor and specific point energy as design parameters in laser powder-bed-fusion (L-PBF) of AlSi10Mg alloy Use of power factor and speci fi c point energy as design parameters in laser powder-bed-fusion (L-PBF) of AlSi10Mg alloy. Mater. Des. doi: https://doi.org/10.1016/j.matdes.2019.108018
[6] Kim, F. H., & Moylan, S. P. (2018). Literature Review of Metal Additive Manufacturing Defects (*No. Advanced Manufacturing Series (NIST AMS)-100-16*).
[7] Taheri, H., Shoaib, M. R. B. M., Koester, L., Bigelow, T., Collins, P. C., & Bond, L. J. (2017). Powder-based additive manufacturing–a review of types of defects, generation mechanisms, detection, property evaluation and metrology. *International Journal of Additive and Subtractive Materials Manufacturing, 1(2), 172.*
[8] Kaufmann, N., Imran, M., Wischeropp, T. M., Emmelmann, C., Siddique, S., & Walther, F. (2016). Influence of process parameters on the quality of aluminium alloy EN AW 7075 using selective laser melting (SLM). *Physics Procedia*, *83*, 918-926.
[9] Picón-Ruiz A., Bereciartua-Pérez, A., Gutiérrez-Olabarria, J.A., Pérez-Larrazabal, J.(2009). La visión artificial en el control de calidad. Desarrollo de un escáner láser tridimensional rotativo. *Dyna, vol. 84, no. 9, pp. 733–742, 2009*.
[10] Thijs, L., Kempen, K., Kruth, J. P., & Van Humbeeck, J. (2013). Fine-structured aluminium products with controllable texture by selective laser melting of pre-alloyed AlSi10Mg powder. *Acta Materialia, 61(5), 1809-1819*.

ACKNOWLEDGEMENTS

We would like to thank European Commission for partially financing this research. The developments have been done in the project BIONIC AIRCRAFT, contract No: H2020-MG-2015-690689, under the H2020 framework programme.